

Beam Based Stochastic Model of the Coverage Probability in 5G Millimeter Wave Systems

Cristian Tatino^{*†}, Ilaria Malanchini[†], Danish Aziz[†], Di Yuan^{*} ^{*}Department of Science and Technology, Linköping University, Sweden

Email: {cristian.tatino, di.yuan}@liu.se [†]Nokia Bell Labs, Stuttgart, Germany

Email: {ilaria.malanchini, danish.aziz}@nokia-bell-labs.com

Abstract

Communications using frequency bands in the millimeter-wave range can play a key role in future generations of mobile networks. By allowing large bandwidth allocations, high carrier frequencies will provide high data rates to support the ever-growing capacity demand. The prevailing challenge at high frequencies is the mitigation of large path loss and link blockage effects. Highly directional beams are expected to overcome this challenge. In this paper, we propose a stochastic model for characterizing beam coverage probability. The model takes into account both line-of-sight and first-order non-line-of-sight reflections. We model the scattering environment as a stochastic process and we derive an analytical expression of the coverage probability for any given beam. The results derived are validated numerically and compared with simulations to assess the accuracy of the model.

I. INTRODUCTION

The ever-growing data rate demand as well as the shortage of mobile frequency resources pose challenges for the upcoming fifth generation (5G) of mobile communications. A way to overcome these problems is to exploit unused frequency bands such as millimeter waves (mm-waves) between 30 to 300 GHz. Mm-waves bring new opportunities, but at the same time raise challenges, e.g., the large path loss caused by higher frequencies dramatically reduces the cell coverage area [1]. The use of highly directional narrow beams with high beamforming gain can help in increasing the cell coverage distance [2], but it requires robustness in procedures such as initial access, beam tracking, mobility management, and handovers.

The main focus of ongoing research related to mm-wave communications is the study of propagation characteristics, channel modeling, beam forming, and medium access control design.

Extensive research is still needed to enable mm-wave communications to be deployed in cellular systems. To this end, we provide a beam based stochastic model for evaluating the coverage probability for any given beam. The analytical expression derived can be then exploited for supporting system level optimization, such as mobility management.

A. Related Works

Communications using mm-waves have been initially investigated for indoor and short range applications, where propagation is facilitated by line-of-sight (LOS) conditions and low-mobility. In [3], the authors propose two algorithms for beam searching, selection and tracking in wireless local area networks. They discretize the set of beams and find, by using iterative search, the best beam pair for the transmitter and the receiver. Similarly, the authors in [4] develop a method that compensates link blockage by switching between the LOS link and a non line-of-sight (NLOS) link, whenever the former is blocked. However, they do not provide any analytical model of the beam coverage and blockage probability.

Lately, the focus has shifted towards the application of mm-waves in outdoor scenarios and cellular systems. In [5], [6], the propagation characteristics of mm-waves are investigated. The study in [5] collects measurements taken in New York at 28 and 38 GHz. Results show that, when a high directional antenna array is used, path loss does not create a significant impediment to the propagation and it is still possible to reach the typical cell coverage of a high density urban environment. Based on the measurements reported in [5], [6] derives a statistical channel model for the path loss, the number of spatial clusters, the angular dispersion, and the outage probability.

Other works exploit stochastic geometry in order to derive statistical channel models and analyze the performance of mm-wave cellular systems. In [7], by proposing a stochastic model for the scattering environment, the authors compute the transmitter-receiver link blockage probability and the probability of coverage both for low frequency and mm-wave cellular networks. However, reflections are ignored. In [8], the authors propose an approach based on random shape theory to provide a statistical characterization of the mm-wave channel and to compute the power delay profile. The model takes into account both the LOS link and all the first-order reflections. Differently from our work, it considers omnidirectional antennas, at both the receiver and the transmitter, and it does not consider any beamforming approach. Leveraging the results in [7], a stochastic approach is adopted also in [9] to provide an analysis of the cell coverage probability

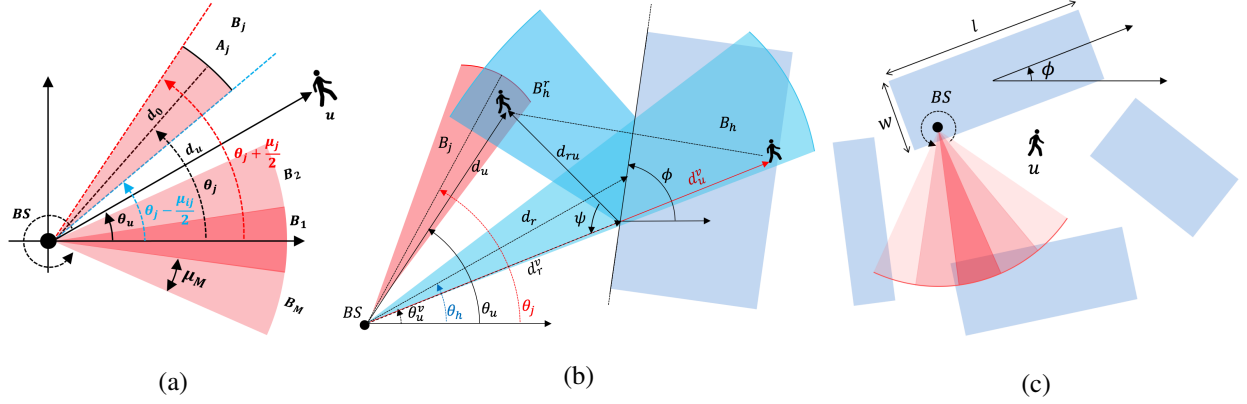


Fig. 1: (a) The BS and a subset of the beams that can be formed, indicated with different color shades. (b) Beam B_j covers directly the user u , whereas beam B_h covers the user u by the reflection B_h^r . (c) A mm-wave cell in an outdoor urban scenario with randomly deployed buildings.

and capacity. The authors demonstrate that, in high cell density conditions, mm-wave networks are able to provide sufficient signal-to-interference-plus-noise ratio (SINR) coverage and higher rate than the low-frequency cellular networks. Compared to previous works, they incorporate a directional beamforming for the SINR computation, at both the base station and the mobile user. However, in this case, reflections are ignored. The same assumption is done in [10], where the authors analyze the impact on the media access control layer design of highly directional communications for mm-waves. Using random shape theory, they investigate initial access and interference management, discussing handover and mobility issues.

B. Our Contributions

In this paper, we propose a beam based model that allows the analysis of the coverage probability and provides a useful tool to accurately investigate the effects of user mobility and beam selection in mm-wave cellular systems.

The main novelty, with respect to the state of the art, lies in the coupling of the following two aspects.

- The model incorporates beamforming, hence it allows to evaluate the coverage probability for any given beam, by taking into account the beam features (i.e., orientation and width) as well as the transmitter-receiver position.

- The model evaluates the coverage probability not only considering the direct beam but also including first-order reflections, which fairly contribute to the coverage probability in NLOS conditions [5].

The rest of the paper is structured as follows. Section II describes the system model and the assumptions. In Section III, we derive the beam coverage probability when blockages and first-order reflections are taken into account. In Section IV, we present a numerical evaluation to validate the accuracy of the model proposed. Section V concludes the paper.

II. SYSTEM MODEL AND ASSUMPTIONS

We target the analysis of beam coverage probability in a cellular scenario. For any cell and user position of interest, the analysis deals with the coverage probability of any given beam. To this end, we consider a cell using mm-wave frequency bands for radio access. The base station (BS) is in the center of the cell and is equipped with a linear array of antennas that can form a discrete set of beams \mathcal{M} of cardinality $|\mathcal{M}|$. Each beam B_j , $j \in \mathcal{M}$, is defined using a sector model and is fully specified by its direction θ_j and width μ_j , as shown in Fig. 1a. Furthermore, we assume the beamforming gain G_j to be a function of the beam width, i.e., $G_j = G(\mu_j)$. The generic user u is fully characterized by its position with respect to the BS, i.e., (θ_u, d_u) , which is given in polar coordinates as shown in Fig. 1a, and is equipped with an omni-directional antenna.

In order to compute the *beam coverage probability*, we evaluate the signal-to-noise ratio (SNR) received by the generic user u from the BS, when a certain beam is used to transmit. Namely, in our model, we assume that the SNR depends on the distance d_u , the carrier frequency f , and the blockage effects caused by the scattering environment. Moreover, we evaluate the SNR considering either the LOS link or a first-order reflection, while excluding the contributions given by links with two or more reflections. This is motivated by the fact that beams reflected more than once arrive at the receiver with a very high path loss (caused by the longer path and a larger reflection loss) and therefore we assume their contributions to the SNR to be negligible. In particular, a first-order reflection B_j^r is generated when the beam B_j hits a building, as shown in Fig. 1b. We assume that beams are narrow enough to be totally reflected and we ignore diffraction and refraction effects. As a result, the beam B_j can cover the user either directly or by its first-order reflection B_j^r . In order to model the scattering environment, as shown in Fig. 1c, we consider buildings with rectangular shape. A building is specified by its center z , length l ,

TABLE I: Summary of the notation

B_j	j^{th} beam
(μ_j, θ_j)	Width and orientation of B_j
A_j	Sector covered by B_j
B_j^r	Reflected beam generated by B_j
(θ_u, d_u)	Polar coordinates of u
(θ_u^v, d_u^v)	Polar coordinates of virtual user u
d_r	Distance between the BS and the obstacle along θ_h
d_r^v	Distance between the BS and the obstacle along θ_u^v
d_{ru}	Distance between the obstacle and u
$\text{SNR}_{B_j u}$	SNR for user u and beam B_j
$\text{SNR}_{B_j u}^D$	SNR for user u and direct beam B_j
$\text{SNR}_{B_j u}^R$	SNR for user u and reflected beam B_j^r
L, W, Φ	Length, width and orientation of an obstacle

width w and orientation ϕ . We assume all these to be independent random variables. Namely, the centers of the buildings Z form a homogeneous Poisson point process (PPP) of density λ . The lengths L and the widths W have probability density function $f_L(l)$ and $f_W(w)$, respectively. The orientations Φ are assumed to be uniformly distributed between $[0, \pi]$. A summary of the notation is reported in Table I.

III. BEAM COVERAGE PROBABILITY

In this section, we compute the *beam coverage probability* of beam B_j , by explicitly considering the dependency between this probability and the beam properties (i.e., orientation and width) as well as the position of the user. We define the event $C_{ju} := \text{SNR}_{B_j u} \geq \Gamma$, where $\text{SNR}_{B_j u}$ is the SNR received by the user u for beam B_j and Γ is a given threshold. Formally, we define the *coverage probability* of beam B_j and the user u , i.e., $P(C_{ju})$, as:

$$P(C_{ju}) = P(\text{SNR}_{B_j u} \geq \Gamma). \quad (1)$$

In order to compute the SNR received by the user at the position (θ_u, d_u) , we distinguish between two cases: the beam B_j covers the user directly or by a reflected beam B_j^r . Given the

assumption that a beam is either not reflected or totally reflected by a building, we consider those two events to be mutually exclusive, i.e., the probability that the same beam covers simultaneously the user both directly and with a reflection is set equal to zero. A beam B_j can cover the user directly if and only if the user u is inside the sector A_j , which is defined by the direction θ_j and the width μ_j as:

$$A_j = \left\{ (\theta, d) \in [0, 2\pi] \times [0, \infty] : |\theta - \theta_j| \leq \frac{\mu_j}{2} \right\}. \quad (2)$$

Therefore, we define the event $D_{ju} := (\theta_u, d_u) \in A_j$ and we denote its complementary event as \bar{D}_{ju} . Thus, according to the law of total probability, $P(C_{ju})$ can be written as:

$$P(C_{ju}) = P(C_{ju} \cap D_{ju}) + P(C_{ju} \cap \bar{D}_{ju}) = P(C_{ju}|D_{ju})P(D_{ju}) + P(C_{ju}|\bar{D}_{ju})P(\bar{D}_{ju}), \quad (3)$$

where the first term of the sum represents the probability that the user is covered directly by the beam, while the second term is the probability to be covered by a reflection.

The first and the second addend of (3) are explicitly derived in Section III-A and in Section III-B, respectively.

A. Direct Beam Coverage Probability

The first term of (3) represents the probability of coverage with direct beam. According to the definition of D_{ju} , we can write the probability $P(D_{ju})$ as:

$$P(D_{ju}) = \begin{cases} 1 & \forall (\theta_u, d_u) \in A_j \\ 0 & \text{otherwise.} \end{cases} \quad (4)$$

Note that the event D_{ju} takes into account only whether the user lies in A_j (or not). In order to incorporate the blockage effect of obstacles, we define LOS_u (NLOS_u) as the event in which the user u is in LOS (NLOS) with respect to the BS. To compute the probability of LOS_u , we use one of the results derived in [7]. Namely, the authors show that (for the very same scattering model adopted here) the number of obstacles between the BS and the user is a random variable O that follows a Poisson distribution with mean:

$$E[O] = \beta d_u + p, \quad (5)$$

where $\beta = [2\lambda(E[L] + E[W])] / \pi$, $p = \lambda E[L]E[W]$ and $E[X]$ indicates the mean of the random variable X . Therefore, the probability that the user is in LOS can be written as follows:

$$P(\text{LOS}_u) = P(O = 0) = e^{-(\beta d_u + p)}. \quad (6)$$

Note that the two events D_{ju} and LOS_u are independent since the former depends only on θ_u and θ_j whereas the latter depends only on d_u . Furthermore, since LOS_u and NLOS_u are complementary events, the first term of (3) can be rewritten as follows:

$$\begin{aligned} P(C_{ju} \cap D_{ju}) = & \\ & P(C_{ju} | D_{ju} \cap \text{LOS}_u) P(D_{ju}) P(\text{LOS}_u) + \\ & P(C_{ju} | D_{ju} \cap \text{NLOS}_u) P(D_{ju}) (1 - P(\text{LOS}_u)). \end{aligned} \quad (7)$$

Moreover, by assumption, refraction is not considered in our model and a signal is completely reflected by an obstacle, hence $P(C_{ju} | D_{ju} \cap \text{NLOS}_u) = 0$.

Let $\{\text{SNR}_{B_j u} | (D_{ju} \cap \text{LOS}_u)\}$ be the received SNR when user u is directly covered by beam B_j in LOS, which we indicate for the rest of the paper as $\text{SNR}_{B_j u}^D$. By applying the Friis' law we can write:

$$\text{SNR}_{B_j u}^D = \frac{P_t G_j G_u c^2}{(4\pi d_u f)^2 P_N}, \quad (8)$$

where P_t is the transmit power, c is the speed of light, G_u is the user beamforming gain, f is the frequency and P_N is the noise power.

To compute the coverage probability, we consider the case in which the SNR is greater than the given threshold Γ . Thus, let us define d_0 as the distance for which $\text{SNR}_{B_j u}^D = \Gamma$; with d_0 and A_j defining the *beam coverage area* as shown in Fig. 1a. Let $\mathbb{1}_{\mathcal{X}}(x)$ be the indicator function, i.e., $\mathbb{1}_{\mathcal{X}}(x) = 1 \ \forall x \in \mathcal{X}$. We can then write the *direct beam coverage probability* as:

$$\begin{aligned} P(C_{ju} \cap D_{ju}) = & P(\text{SNR}_{B_j u}^D \geq \Gamma) P(D_{ju}) P(\text{LOS}_u) = \\ & \mathbb{1}_{[\theta_j - \frac{\mu_j}{2}, \theta_j + \frac{\mu_j}{2}] \times [0, d_0]}(\theta_u, d_u) e^{-(\beta d_u + p)}. \end{aligned} \quad (9)$$

B. Reflected Beam Coverage Probability

We now investigate the probability of being covered by a first-order reflection. In general, B_j can generate different reflections, which depend on the position and orientation of the building

that is hit by the beam. In order to compute them, we assume the specular reflection law, i.e., the incident angle is assumed to be equal to the reflected one. Moreover, given the narrow beam assumption, we consider only the case in which the entire beam hits only one side of an obstacle (see Fig. 1b). Furthermore, the side of the building that is hit by the beam generates a straight line that divides the space in two half-planes, as shown in Fig. 1b. Thus, we compute the symmetric point (θ_u^v, d_u^v) of the user position with respect to this line, which we call *virtual user position*.

The user u is covered by a first-order reflected beam if the two events R_{ju} and LOS_u^R jointly hold, where $R_{ju} := \{\theta_u^v \in A_j\} \cap \{d_u^v \geq d_r^v\}$ and LOS_u^R is the event in which the user u is in LOS with respect to the obstacle. Note that d_r^v is the distance between the BS and the obstacle along the direction identified by θ_u^v , as shown in Fig. 1b. By considering that the events \bar{D}_{ju} , R_{ju} and LOS_u^R are independent, we can write

$$P(C_{ju}|\bar{D}_{ju}) = P(\text{SNR}_{B_j u}^R \geq \Gamma)P(R_{ju})P(\text{LOS}_u^R), \quad (10)$$

where $\text{SNR}_{B_j u}^R$ is the received SNR when beam B_j is reflected once by an obstacle. By applying the Friis' formula, we obtain

$$\text{SNR}_{B_j u}^R = \frac{P_t G_j^r G_u c^2}{(4\pi d_u^v f)^2 \sigma P_N}, \quad (11)$$

where the beamforming gain of the reflected beam is $G_j^r = G_j$ and σ is the reflection loss. Thus, we can derive the distance for which $\text{SNR}_{B_j u}^R = \Gamma$ as $d_0^v = \frac{d_0}{\sigma}$.

The events $\{\text{SNR}_{B_j u}^R \geq \Gamma\}$, R_{ju} , and LOS_u^R and their respective probabilities depend on, e.g., d_u^v , θ_u^v , and d_r^v (which is the distance between the user and the obstacle). Those in turn depends on the beam properties and the user position, which are both given, and on the distance of the first obstacle from the BS, d_r , and its orientation ϕ , see Fig. 1b. According to the stochastic model adopted for the scattering environment, those variables are described by probability density functions $f_{D_r}(d_r)$ and $f_\Phi(\phi)$, respectively. The latter is assumed to be uniformly distributed between $[0, \pi]$, whereas

$$f_{D_r}(d_r) = \delta(d_r) (1 - e^{-p}) + (1 - \delta(d_r)) \beta e^{-(\beta d_r + p)} U(d_r), \quad (12)$$

where $\delta(r)$ is the Dirac delta function, i.e., $\delta(r) = 1$ for $r = 0$ and 0 otherwise, and $U(r)$ is the Heaviside step function. The details of the computation can be found in Appendix A.

$$P(C_{ju} \cap \bar{D}_{ju}) = (1 - P(D_{ju})) \times \int_0^\pi \int_0^\infty \mathbb{1}_{[\theta_j - \frac{\mu_j}{2}, \theta_j + \frac{\mu_j}{2}] \times [d_r^v, \frac{d_0}{\sigma}]}(\theta_u^v(r, \alpha), d_u^v(r, \alpha)) P(\text{LOS}_u^R | r, \alpha) \\ (\delta(r) (1 - e^{-p}) + (1 - \delta(r)) \beta e^{-(\beta r + p)} U(r)) \frac{1}{\pi} dr d\alpha \quad (13)$$

To derive the final expression of the reflected beam coverage probability, reported in (13), we condition all terms of (10) on D_r and Φ . The product of the first two (conditioned) terms of (10) leads to the indicator function in (13), whereas the $P(\text{LOS}_u^R | D_r = d_r, \Phi = \phi)$ is shown in Appendix B.

IV. NUMERICAL EVALUATION

In this section, we present the results of our study on the *beam coverage probability*. We assess the validity of our model by comparing the numerical results for $P(C_{ju})$, computed using the analytical model, with simulation results. We used Matlab to compute numerically (13), hence (3), as well as to obtain the simulations results. It is important to note that in the simulation setup, we remove the assumption that a beam can hit only one side of an obstacle and we allow the beam to hit several obstacles (and sides), hence generating several reflections. Clearly, this makes the simulation environment more realistic, but also leads to some gap between the model and the simulation results, as shown later.

A. Simulation Setup

We consider a simulation area of $500 \times 500 \text{ m}^2$ and we place the base station in the centre of the area. We independently generate 10,000 instances by dropping the buildings randomly, according to a PPP of density λ . In order to obtain a comprehensive performance evaluation, hereafter, we vary several parameters, such as beam width and orientation, building density, and position of the user. The parameters that are fixed are: $P_t = 30 \text{ dBm}$ (as the experiments in [6]), $P_N = -85 \text{ dBm}$, $f = 30 \text{ GHz}$, and $\Gamma = 1$, i.e., 0 dB . W and L are characterized by uniform distribution between $[30, 50]$ and $[40, 60]$ (in meters), respectively. The reflection loss, which depends on several factors, e.g., angle of incidence on the obstacle, frequency, materials of the wall, is set to $\sigma = 3 \text{ dB}$ (as proposed in [8]), which means that half of the power is lost when the beam hits a building. Moreover, the results consider two different beam widths: $\mu_{ij} = 10^\circ$

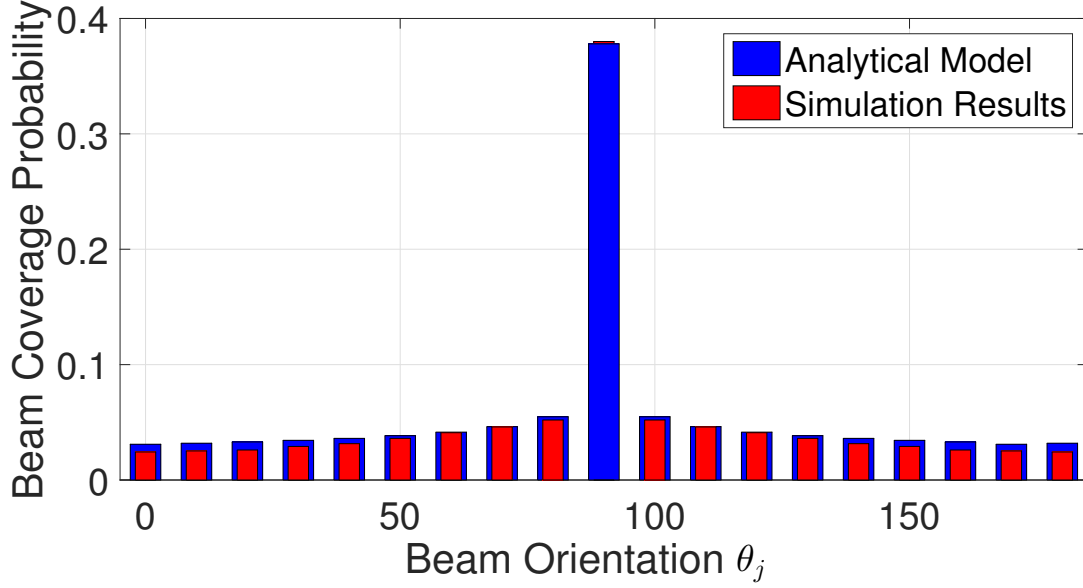


Fig. 2: The beam coverage probability computed for different non-overlapping beams with width $\mu_j = 10^\circ$.

and $\mu_{ij} = 30^\circ$. Since the gain depends on the beam width itself, we set $G(10^\circ) = 36$ dBi and $G(30^\circ) = 12$ dBi, which are assumed constant inside A_j and equal to 0 elsewhere. Moreover, we assume that $G_u = 1$ dBi.

B. Results

Fig. 2 shows the beam coverage probability when varying the beam orientation θ_j . The user position is $(90^\circ, 50 \text{ m})$, the building density is $\lambda = 0.0002$ buildings/m², and the beam width is $\mu_j = 10^\circ$. First, we observe that analytical and simulation results are very close to each other, validating the proposed model. Furthermore, we see that $P(C_{ju})$ decreases as the difference between the angular coordinate of the user, θ_u , and the beam direction, θ_j , increases. In particular, the coverage probability of the direct beam ($\theta_j = 90^\circ$) is much larger than the ones obtained from reflected beams. Namely, when the beam direction moves away from the user angular coordinate, the path between the user and the obstacle becomes longer. Consequently, both the received SNR and the probability that the user is in LOS with respect to that obstacle decrease. Similar results have been obtained for different beam widths, but they are not reported for the sake of space.

Although the contribution to the coverage probability of the non-direct beams is smaller compared to the direct one, the aggregation of all of them can have a significant impact on the

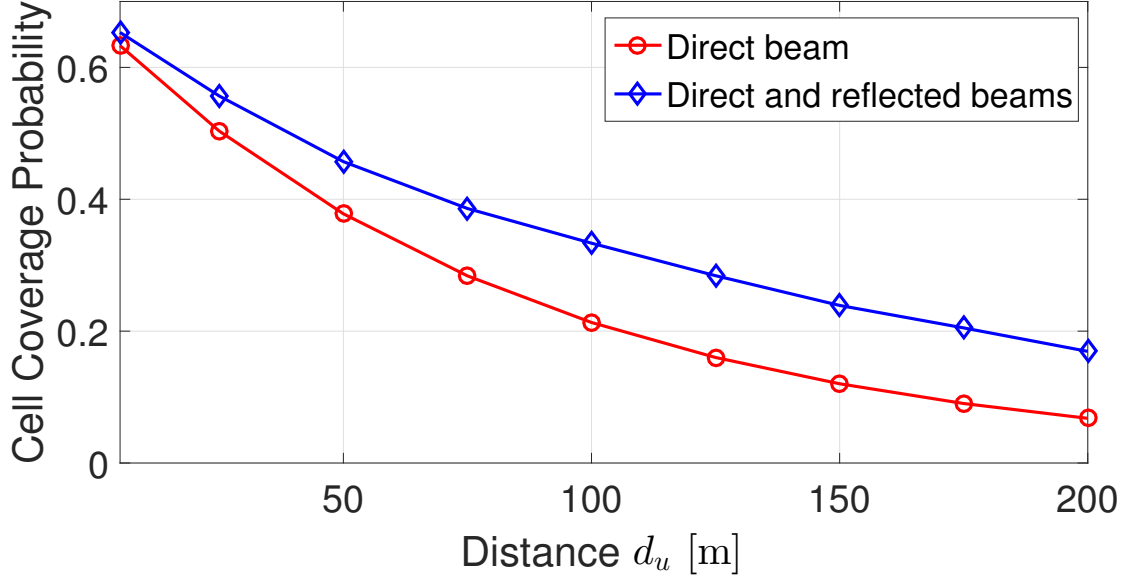


Fig. 3: Comparison between the cell coverage probability when considering only the direct beam and when including all possible reflected beams.

cell coverage probability. In Fig. 3, we compare the simulated cell coverage probability when only the direct beam is considered and when reflections are also included. Namely, in the latter case, the cell coverage probability is defined as the probability that at least one beam covers the user. We use the same parameters of Fig. 2, but we vary the user distance d_u . We observe that the cell coverage probability of the direct beam decreases faster in comparison to that with reflected beams. Moreover, the contribution of the reflections become more evident as the user distance increases. Similar conclusions can be drawn from Fig. 4, in which we show the beam coverage probability, varying the user distance d_u , for the direct beam and two reflected beams, when $\lambda = 0.0002$ buildings/m². In this case, the angular coordinate of the user is $\theta_u = 90^\circ$ and the direct beam is the one with orientation $\theta_j = \theta_u$. Furthermore, we select two reflected beams: a first beam with $\theta_j = 95^\circ$ and $\mu_j = 10^\circ$, and a second beam with $\theta_j = 105^\circ$ and $\mu_j = 30^\circ$. In both cases, the reflected beam is chosen such that the user is placed at the border of the beam coverage angle, which corresponds to the best non-direct beam (in terms of beam coverage probability). We observe that the direct beam coverage probability decreases rapidly as d_u increases, whereas the reflected beam coverage probability remains almost constant. Fig. 4 further validates our model, reported with solid lines, with respect to simulations results, reported

with dashed lines. In particular, the divergence between model and simulation results, for the reflected beam curves, increases with d_u . This is due to the assumption (made in the analytical model, but not in the simulation setup) that the reflected beam hits only one side of the same building and is totally reflected, proving that our model is more accurate for narrow beams.

The validity of the model is shown also in Fig. 5, where we compare the beam coverage probability when the building density λ increases, for a fixed user position (90° , 50 m) and the same beam set assumed in Fig. 4. In general, we observe that the analytical model matches well the simulation results. Moreover, the coverage probability of the direct beam decreases as the density λ increases, whereas the coverage probability of the reflected beams has a non-monotonic behavior. Namely, it increases from zero (when there are no buildings, hence no reflections) reaching a maximum for a given building density, and then decreases again. This behaviour is due to twofold effect that the building density has on the reflections. On one hand, increasing the building density corresponds to increasing the possibilities of generating reflections, which enhances the beam coverage probability. On the other hand, increasing the building density reduces the probability of LOS between the position of the first obstacle and the user, which decreases the beam coverage probability.

Finally, both Fig. 4 and Fig. 5 show that, by increasing the beam width, we can enhance the coverage probability of reflected beams (i.e., when there are NLOS conditions). This is due to the fact that the reflection of wider beams can cover a larger area and thus increase the probability of covering the user. This is an important outcome of our analysis, which suggests that width should be trade off between narrow beams, which are very good in LOS conditions, and wider beams, which can provide good coverage probability in NLOS conditions.

V. CONCLUSION

In this paper, we propose a beam based stochastic model for evaluating the beam coverage probability in mm-wave cellular systems. We model the scattering environment as a stochastic process and we derive an analytical expression valid for any given beam with respect to a given user position. The proposed model is able to capture the dependency of the beam coverage probability on various parameters, such as user position, beam orientation and width, and building density.

In general, the analytical model matches well the simulation results, especially for narrow beams. Furthermore, we show that, although the highest coverage probability is provided by

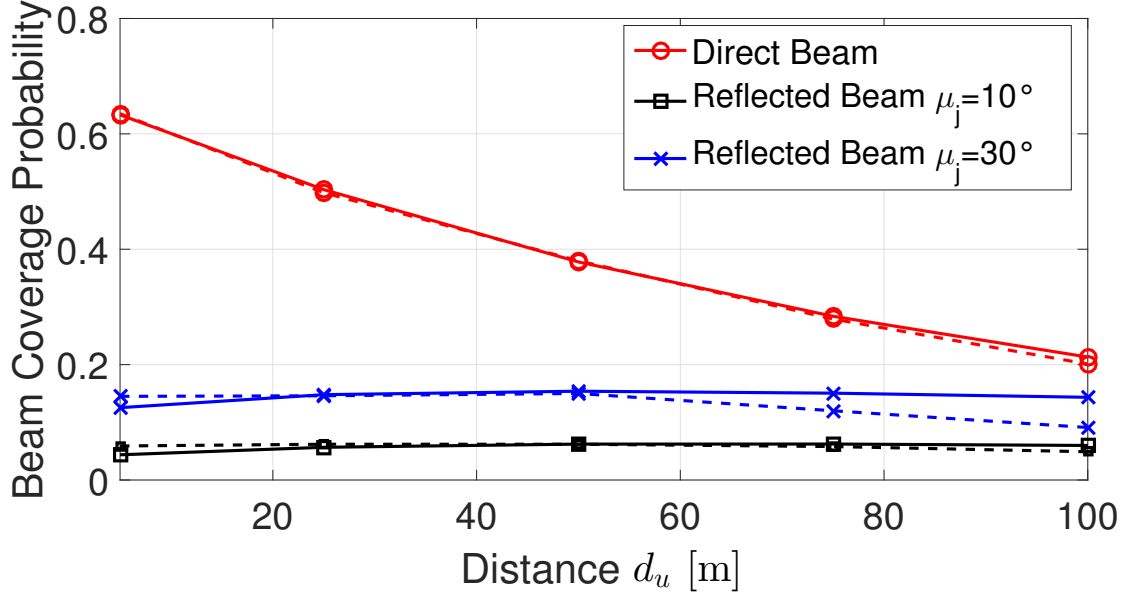


Fig. 4: Comparison between the analytical model (solid line) and simulation results (dashed line) of the direct and reflected beam coverage probability with varying user distance d_u .

the direct beam, reflections can fairly contribute to it, especially for larger user distances, i.e., when the LOS probability dramatically decreases. Moreover, the results show a non-monotonic behaviour of the reflected beam coverage probability with respect to the building density, which suggests that an optimal building density exists for NLOS conditions. Finally, we observe that increasing the beam width is a good strategy to improve the beam coverage probability in NLOS conditions.

Future work will further investigate the coverage properties due to reflections, and extend the model to improve the accuracy for wider beams. Furthermore, we will investigate how the proposed model can be used for network optimization, e.g., mobility management, in mm-wave systems.

VI. APPENDIX A

Hereafter, we derive the probability density function (PDF) of the distance of the first obstacle from the base station along a given direction, i.e., $f_{D_r}(d_r)$. Recall that the distribution of the total number of obstacles along a particular segment of distance d_r is a Poisson random variable

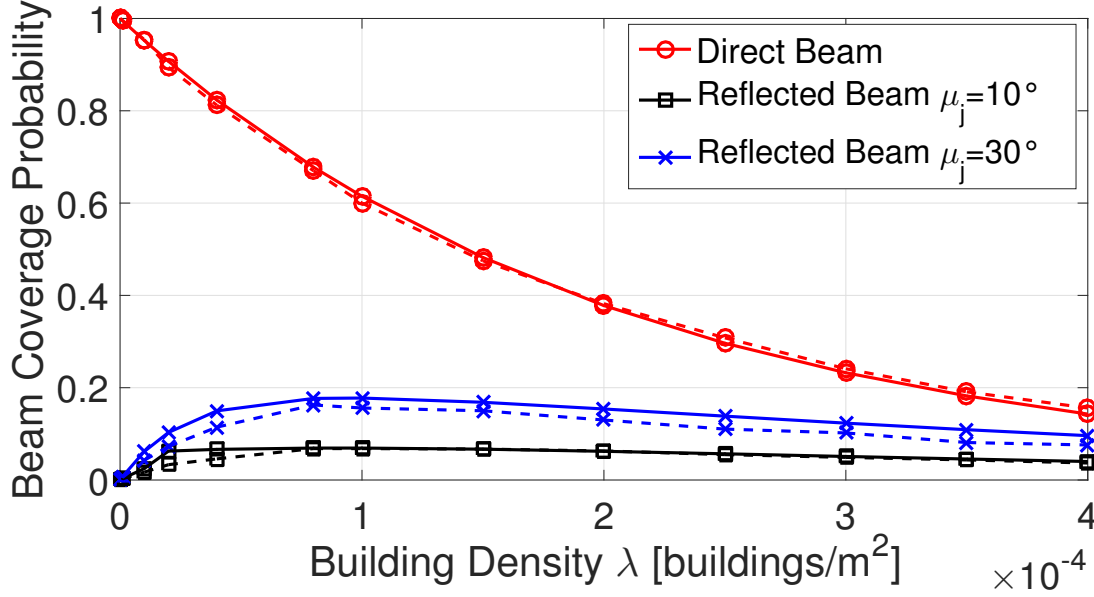


Fig. 5: Comparison between the analytical model (solid line) and simulation results (dashed line) of the direct and reflected beam coverage probability with varying building density λ .

O with mean defined in (5), cf. [7]. Therefore, the cumulative density function (CDF) $F_{D_r}(d_r)$ can be written as

$$F_{D_r}(d_r) = P(D_r \leq d_r) = 1 - P(D_r \geq d_r) = 1 - P(O(d_r) = 0) = 1 - e^{-(\beta d_r + p)}. \quad (14)$$

Since the CDF is equal to 0 for $d_r < 0$, it has a discontinuity in zero caused by the non-zero dimension of the obstacles. Therefore, to compute the PDF $f_{D_r}(d_r)$ we separate the two cases, i.e., $d_r = 0$ and $d_r > 0$. Then we obtain

$$f_{D_r}(d_r) = \begin{cases} 1 - P(O(0) = 0) = 1 - e^{-p} & d_r = 0 \\ \frac{dF_{D_r}(d_r)}{dd_r} = \beta e^{-(\beta d_r + p)} & d_r > 0. \end{cases} \quad (15)$$

VII. APPENDIX B

One can easily see that the event LOS_u^R is strongly correlated to the distance, d_r , between the BS and the first obstacle. For the sake of space we skip the details and we directly report the

derived approximation of $P(\text{LOS}_u^R | D_r = d_r, \Phi = \phi)$, which is

$$P(\text{LOS}_u^R | D_r = d_r, \Phi = \phi) = \begin{cases} \min(1, e^{-\beta d_{ru} + q}) & 0 \leq \psi \leq \frac{\pi}{2}, d_r \geq d_{ru} \\ \min(e^{-\beta(d_{ru} - d_r)}, e^{-\beta d_{ru} + q}) & 0 \leq \psi \leq \frac{\pi}{2}, d_r \leq d_{ru} \\ e^{-\beta d_{ru}} & \frac{\pi}{2} \leq \psi \leq \pi \end{cases} \quad (16)$$

where d_{ru} is the distance between the user and the obstacle, $q = \lambda \cot(\psi)(E[L^2] + E[W^2])/2$ and ψ is the angle formed by the reflection and directly depends on ϕ , as shown in Fig. 1b. $E[L^2]$, and $E[W^2]$ are the second moments of the length and width of the obstacles, respectively.

ACKNOWLEDGMENT

The authors would like to thank Dr. Vangelis Angelakis and Dr. Nikolaos Pappas for the insightful discussions.

This project has received funding from the European Union's Horizon 2020 research and innovation programme under the Marie Skłodowska-Curie grant agreement No. 643002.

REFERENCES

- [1] S. Rangan, T. S. Rappaport, and E. Erkip, "Millimeter-wave cellular wireless networks: potentials and challenges," *Proceedings of the IEEE*, vol. 102, no. 3, pp. 366–385, March 2014.
- [2] W. Roh, J. Y. Seol, J. Park, B. Lee, J. Lee, Y. Kim, J. Cho, K. Cheun, and F. Aryanfar, "Millimeter-wave beamforming as an enabling technology for 5G cellular communications: theoretical feasibility and prototype results," *IEEE Communications Magazine*, vol. 52, no. 2, pp. 106–113, February 2014.
- [3] J. Wang, "Beam codebook based beamforming protocol for multi-Gbps millimeter-wave WPAN systems," *IEEE Journal on Selected Areas in Communications*, vol. 27, no. 8, pp. 1390–1399, October 2009.
- [4] X. An, C.-S. Sum, R. Prasad, J. Wang, Z. Lan, J. Wang, R. Hekmat, H. Harada, and I. Niemegeers, "Beam switching support to resolve link-blockage problem in 60 GHz WPANs," in *IEEE 20th International Symposium on Personal, Indoor and Mobile Radio Communications*, September 2009, pp. 390–394.
- [5] T. Rappaport, S. Sun, R. Mayzus, H. Zhao, Y. Azar, K. Wang, G. Wong, J. Schulz, M. Samimi, and F. Gutierrez, "Millimeter wave mobile communications for 5G cellular: It will work!" *IEEE Access*, vol. 1, pp. 335–349, May 2013.
- [6] M. R. Akdeniz, Y. Liu, M. K. Samimi, S. Sun, S. Rangan, T. S. Rappaport, and E. Erkip, "Millimeter wave channel modeling and cellular capacity evaluation," *IEEE Journal on Selected Areas in Communications*, vol. 32, no. 6, pp. 1164–1179, June 2014.
- [7] T. Bai, R. Vaze, and R. W. Heath, "Analysis of blockage effects on urban cellular networks," *IEEE Transactions on Wireless Communications*, vol. 13, no. 9, pp. 5070–5083, September 2014.
- [8] N. A. Muhammad, P. Wang, Y. Li, and B. Vucetic, "Analytical model for outdoor millimeter wave channels using geometry-based stochastic approach," *IEEE Transactions on Vehicular Technology*, vol. 66, no. 2, pp. 912–926, 2017.

- [9] T. Bai and R. W. Heath, "Coverage and rate analysis for millimeter-wave cellular networks," *IEEE Transactions on Wireless Communications*, vol. 14, no. 2, pp. 1100–1114, February 2015.
- [10] H. S. Ghadikolaei, C. Fischione, G. Fodor, P. Popovski, and M. Zorzi, "Millimeter wave cellular networks: A MAC layer perspective," *IEEE Transactions on Communications*, vol. 63, no. 10, pp. 3437–3458, October 2015.